Archives of Oral Biology 124 (2021) 105061

Contents lists available at ScienceDirect

Archives of Oral Biology

journal homepage: www.elsevier.com/locate/archoralbio

FNDC5/irisin is expressed and regulated differently in human periodontal ligament cells, dental pulp stem cells and osteoblasts

Yang Yang [a], Helen Pullisaar [b], Maria A. Landin [a], Catherine Anne Heyward [c], Maria Schröder [a], Tianxiang Geng [a], Maria Grano [d], Janne Elin Reseland [a,*]

[a] Department of Biomaterials, Faculty of Dentistry, University of Oslo, Oslo, Norway
[b] Department of Orthodontics, Faculty of Dentistry, University of Oslo, Oslo, Norway
[c] Oral Research Laboratory, Faculty of Dentistry, University of Oslo, Oslo, Norway
[d] Department of Emergency and Organ Transplantation, University of Bari, Bari, Italy

ARTICLE INFO

Keywords:
FNDC5
Irisin
Human periodontal ligament cell
Human dental pulp stem cell
Human osteoblast

ABSTRACT

Objective: To examine the expression and regulation of fibronectin type III domain-containing protein 5/irisin (FNDC5/irisin) in primary human periodontal ligament (hPDL) cells, dental pulp stem cells (hDPCs) and osteoblasts (hOBs).

Methods: FNDC5/irisin was identified in sections of paraffin embedded rat maxillae, cryo-sections of 3D cultured spheroids hPDL cells, hDPCs and hOBs, 2D cultured hPDL cells, hDPCs and hOBs by immunohistochemistry. The expression of FNDC5/irisin was identified by qPCR, followed by sequencing of the qPCR product. Regulation of FNDC5/irisin expression in hPDL cells, hDPCs and hOBs were evaluated after administration of different concentrations of irisin and all-trans retinoic acid (ATRA). qPCR and ELISA were used to identify expression and secretion of FNDC5/irisin in odontoblast-like differentiation of hDPCs.

Results: FNDC5/irisin was confirmed to be present in rat periodontium and dental pulp regions, as well as in 2D and 3D cultured hPDL cells, hDPCs and hOBs. BLAST analyses verified the generated nucleotide alignments matched human FNDC5/irisin. FNDC5/irisin gene expression was enhanced during odontoblast-like differentiation of hDPCs whereas the secretion of the protein was decreased compared to control. The protein signals in rat periodontal and pulpal tissues were higher than that of alveolar bone, and the expression of FNDC5/irisin was differently regulated by recombinant irisin and ATRA in hPDL cells and hDPCs compared to hOBs.

Conclusions: FNDC5/irisin expression was verified in rodent periodontium and dental pulp, and in hPDL cells, hDPCs and hOBs. The FNDC5/irisin expression was regulated by recombinant irisin and ATRA. Finally, expression and secretion of FNDC5/irisin were affected during odontoblast-like differentiation of hDPCs.

1. Introduction

Irisin is a newly identified polypeptide hormone that is proteolytically cleaved from its precursor fibronectin type III domain-containing protein 5 (FNDC5), released into circulation in response to physical activity, and identified to be present in skeletal muscle and blood plasma (Boström et al., 2012). The systematic location and expression of FNDC5/irisin in other human tissues was first comprehensively examined by Aydin et al., who identified FNDC5/irisin to be expressed in perimysium, endomysium, testis, pancreas, spleen, liver, brain, stomach and cardiac tissues. They also defined the nerve sheaths spreading within human skeletal muscles to be the main producers of FNDC5/irisin (Aydin, Kuloglu et al., 2014). Nonetheless, the expression of FNDC5/irisin within oral tissues has only been ascertained in 3 main salivary glands, which are parotid, sublingual and submandibular glands (Aydin, Aydin et al., 2014, 2013). The role of FNC5/irisin in these oral tissues remains unclear, however, *in vitro* studies have demonstrated that administration of recombinant irisin enhanced cell growth, migration and extracellular matrix deposition in both primary human periodontal ligament cells and osteoblasts (Pullisaar et al., 2019),

Abbreviations: hPDL cells, human periodontal ligament cells; hDPCs, human dental pulp stem cells; hOBs, human osteoblasts; FNDC5, fibronectin type III domain-containing protein 5; ATRA, all-trans retinoic acid.

* Corresponding author.
E-mail address: j.e.reseland@odont.uio.no (J.E. Reseland).

https://doi.org/10.1016/j.archoralbio.2021.105061
Received 31 July 2020; Received in revised form 2 January 2021; Accepted 10 January 2021
Available online 23 January 2021
0003-9969/© 2021 The Author(s). Published by Elsevier Ltd. This is an open access article under the CC BY license (http://creativecommons.org/licenses/by/4.0/).

whereas recombinant irisin was found to reduce proliferation and promote mineral deposition and differentiation of an immortalized mouse cementoblast cell line (Zhu et al., 2020). Hence, it would be of interest to investigate if FNDC5/irisin is expressed in oral tissues and cells supporting tooth attachment.

Periodontium is a sophisticated tooth-supporting apparatus composed of four important tissues - gingiva, cementum, alveolar bone and periodontal ligament (PDL) (Bartold, 1991). PDL is a connective tissue situated between tooth root cementum and alveolar bone, and is constantly exposed to mechanical stimuli from surrounding tissues and physiological functions such as mastication and speech (Ozaki, Kaneko, Podyma-Inoue, Yanagishita, & Soma, 2005). PDL together with cementum and alveolar bone form a dynamic and biomechanically active fibrous joint called bone-PDL-tooth complex, which comprises two adaptive functional interfaces, namely PDL-bone and PDL-cementum. When loaded, the mechanical load can stimulate PDL cells residing at the multiple sites of the complex to induce an array of biological events such as osteogenesis, osteoclastogenesis and inflammation (Feller et al., 2015; Lin et al., 2017). Based on the fact that FNDC5/irisin is activated in response to mechanical loading, we thus hypothesize that FNDC5/irisin is likely to be expressed in PDL cells because PDL is frequently subject to mechanical stimuli.

Dental pulp is a soft connective tissue located in a hard chamber consisting of dentine, enamel and cementum, and contains blood vessels, nerves and mesenchymal tissue, and is essential in tooth development and maintenance (Chalisserry, Nam, Park, & Anil, 2017). The dental pulp possesses a mesenchymal stem cell population, which is referred to as dental pulp stem cells (DPCs) (Nuti, Corallo, Chan, Ferrari, & Gerami-Naini, 2016). They have multi-lineage differentiation potential, and can differentiate towards osteoblasts, odontoblasts, adipocytes, chondrocytes and neural-like cells, which grant the DPCs a pivotal role in dental tissue regeneration (Nuti et al., 2016). Since FNDC5/irisin has been reported to be involved in neural and cardiomyocyte differentiation of mouse embryonic stem cells (Forouzanfar et al., 2015; Rabiee et al., 2014), we also speculate that FNDC5/irisin may be expressed in DPCs and involved in their differentiation.

Therefore, the primary aim of the present research is to study possible expression of FNDC5/irisin within rat periodontal ligament, dental pulp, alveolar bone, commercially available hPDL cells, hDPCs and hOBs. Further, to examine the regulation of FNDC5/irisin expression within these cells and clarify if odontoblast-like differentiation could affect FNDC5/irisin expression and secretion in hDPCs.

2. Materials and methods

2.1. Histology of oral tissues from rats

In order to verify the expression of irisin in rats' periodontal and dental pulp tissues, sections of the dental tissues around upper first molars of 3 male, 12-week-old Sprague-Dawley rats were used. The rat samples were acquired from a previous study and the preparation and embedding of the tissues are described elsewhere (Villa et al., 2015). The experiment was approved by the National Animal Research Authority, in accordance with the Animal Welfare Act of January 1, 2010, Section 13 and the Regulation on Animal Experimentation of January 15, 1996.

Tissues were sectioned into 5 μm-thickness bucco-lingual cross-section cuts parallel to the long axis of upper first molars and mounted onto glass slides. Tissue sections were deparaffinized, rehydrated and antigen-retrieved by heating in Tris-EDTA buffer (10 mM Tris base, 1 mM EDTA solution, 0.05 % Tween 20, PH 9.0) in a microwave oven for 10 min prior to immunofluorescence staining.

2.2. 2D cell culture

hPDL cells (Lonza, Walkersville, MD, USA) and hDPCs (Lonza, Walkersville, MD, USA) were cultured in Dulbecco's modified Eagle's medium (Sigma-Aldrich, Saint-Louis, Missouri, USA) supplemented with 200 mM GlutaMAX (Gibco, Thermo Fisher Scientific, Waltham, MA, USA), 10 % fetal bovine serum and 100 μg/mL penicillin/100 IU μg/mL streptomycin (Lonza, Allendale, NJ, USA) at 37 °C in a humid atmosphere of 5 % CO_2. The cells were used in passages 4–8.

Human osteoblasts (hOBs) (Lonza, Walkersville, MD, USA) were cultured in osteoblast culture medium supplemented with 10 % fetal bovine serum, 0.1 % gentamicin sulfate, amphotericin-B and ascorbic acid (Lonza, Walkersville, MD, USA) at 37 °C in a humid atmosphere of 5 % CO_2. The hOBs in passages 4–8 were used.

To test whether the expression of FNDC/irisin was regulated. hPDL cells, hDPCs and hOBs were seeded in 12-well culture plates at the density of 5×10^3 cells/cm^2, 3.5×10^3 cells/cm^2 and 6.0×10^3 cells/cm^2, respectively. At 80 % confluence, 10 ng/mL and 100 ng/mL of recombinant irisin (Adipogen, Liestal, Switzerland), or 1 μM and 10 μM of all-trans retinoic acid (ATRA) (Sigma-Aldrich, Saint-Louis, Missouri, USA) (Amengual et al., 2018) were administrated, respectively. The control groups for each of the treatment were incubated with equal volumes of sterile milliQ water (control for recombinant irisin) or DMSO (control for ATRA). The cells were maintained in a humidified incubator supplemented with 5 % CO_2 at 37 °C for 3 days prior to harvest and further analyses.

For immunofluorescence analysis, hPDL cells, hDPCs and hOBs were fixed in 4 % paraformaldehyde (PFA) for 15 min and preserved in PBS at 4 °C until use.

Dexamethasone (10^{-8} M; Sigma-Aldrich, Saint-Louis, Missouri, USA) was administrated to confluent hDPCs to induce differentiation towards odontoblast-like cells. The corresponding control cells received equal amounts of the diluent 0.1 % ethanol, without dexamethasone. Cells were cultured for 14 days, culture medium were refreshed 24 h before harvest and both mRNA and cell culture medium were collected at each time point (1, 3, 7 and 14 days) and stored at -80 °C prior to qPCR and ELISA analyses, respectively.

2.3. 3D cell culture

Spheroids were generated from approximately 6.5×10^6 hPDL cells, 4.6×10^6 hDPCs and 7.8×10^6 hOBs in individual disposable 10 mL vessel using the rotational 3D cell culture system from CelVivo (Blommenslyst, Denmark). The culture media was replaced every 3 days. After 14 days of 3D culture, spheroids of different sizes were generated, and the largest spheroids (diameter between 0.5–1 mm) were fixed in 4 % PFA for 30 min, transferred to PBS and stored at 4 °C prior to further analyses.

The fixed spheroids were embedded in optimal cutting temperature (OCT) compound (Leica, Buffalo Grove, IL, USA), and frozen at −20 °C. Serial sections of the spheroids (7 μm) were obtained using a CryoStar™ NX70 Cryostat (Thermo Fisher Scientific, Kalamazoo, MI, USA) and mounted onto glass slides and stored at −20 °C.

2.4. mRNA extraction

Dynabeads™ mRNA DIRECT™ Purification Kit (Thermo Fisher Scientific, Carlsbad, CA, USA) was used for mRNA extraction. Briefly, 2D cultured hPDL cells, hDPCs and hOBs were washed in cold PBS and lysed, and the mRNA was isolated using magnetic beads according to manufacturer's instructions. mRNA was separated from the beads by heat treatment (80 °C for 2 min) and quantified using a nano-drop spectrophotometer (ND-1000, Thermo Scientific, Wilmington, DE, USA, with software version 3.3.1.).

2.5. cDNA synthesis and qPCR

cDNA was synthesized using 2 μg of mRNA with first strand cDNA synthesis kit (Thermo Fisher Scientific, Waltham, MA, USA) according to

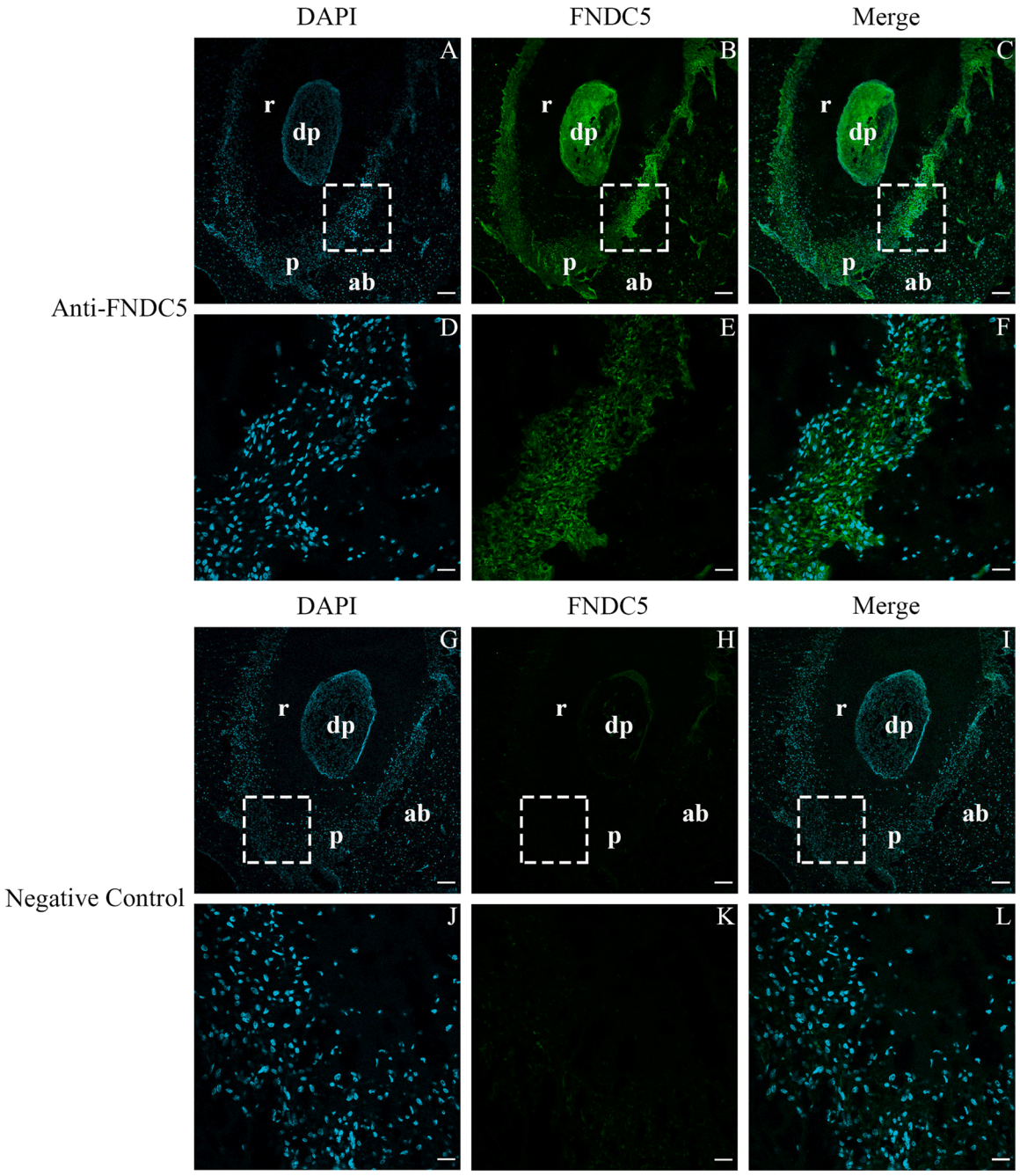


Fig. 1. Immunofluorescence detection of FNDC5 in rats' oral tissues. Histological sections of periodontium and dental pulp of upper first molars were analyzed by immunofluorescence staining for FNDC5 (B, C, E and F). Negative control was not treated with anti-FNDC5 primary antibody (H, I, K and L). Nuclei were counterstained with DAPI (A, C, D, F, G, I, J and L). Merged images of DAPI and FNDC5 are shown in C, F, I and L. The white boxed areas are shown at a higher magnification (D, E, F, J, K and L). The images are representative of the respective groups. Abbreviations: r for root, dp for dental pulp, p for periodontium, ab for alveolar bone. Scale bars in A, B, C, G, H and I represent 100 μm, scale bars in D, E, F, J, K and L represent 25 μm.

manufacturer's instructions. qPCR was conducted in a CFX384 TouchReal-Time PCR Detection System (Bio Rad, Hercules, California, USA) using IQ SYBR Green Supermix (Bio Rad, Hercules, California, USA) in a total volume of 20 μL (1 ng cDNA). The $^{\Delta\Delta}$Ct method (Livak & Schmittgen, 2001) was utilized to calculate the relative mRNA levels of the genes that were normalized to glyceraldehyde-3-phosphate dehydrogenase (GAPDH). The primers used for qPCR were synthesized by Invitrogen (Thermo Fisher Scientific, Carlsbad, CA, USA), and are as follows: GAPDH, forward 5′-CTCTGCTCCTCCTGTTCGAC-3′, reverse 5′-ACGACCAAATCCGTTGACTC-3′; FNDC5, forward 5′-CTCTCCACTG CCCCTTTCTG-3′, reverse 5′-GCAGATGTCCACCTCTTCCC-3′.

2.6. DNA -electrophoresis

DNA electrophoresis of the qPCR products were performed using the FlashGel System (Lonza, Allendale, NJ, USA) according to the producers' instructions. A mixture of 5 μL of DNA marker, 5 μL of qPCR products from 2D cultured hPDL cells, hDPCs and hOBs, and 1 μL of 6 X DNA loading dye (Thermo Fisher Scientific, Waltham, MA, USA) were loaded on a 2 % agarose Tris-acetate-EDTA (TAE) gel containing 0.01 % SYBR safe DNA gel stain (Thermo Fisher Scientific, Waltham, MA, USA). Images of the bands in the gels were captured through the built-in camera within the FlashGel System.

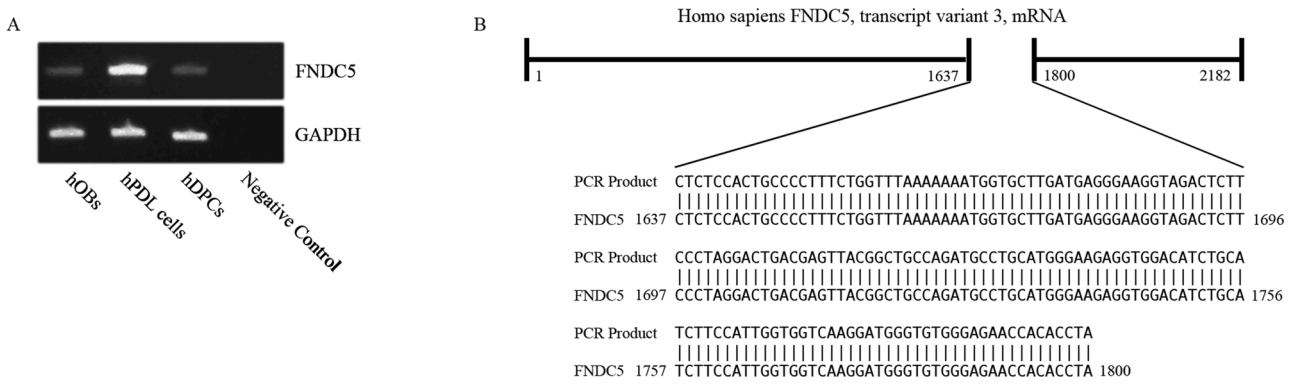


Fig. 2. Expression of FNDC5 in hPDL cells, hDPCs and hOBs. The images are representative of the respective groups. H_2O was used as negative control (A). The BLAST search and DNA sequencing analysis. The alignments of deduced amino acid sequences from hPDL cells qPCR products matched Homo sapiens FNDC5, transcript variant 3, mRNA sequence GenBank ID: NM_001171940.2, length: 2182, range: 1637 to 1800 (B).

2.7. Sequencing of PCR products

Aliquots (5 μl) of PCR product from 2D cultured hPDL cells were purified with 2 μl ExoSAP-IT Express PCR Cleanup Reagents (Thermo Fisher Scientific, Waltham, MA, USA), and diluted with DNAse-free water (1:5). The samples were sequenced at the MRC Protein Phosphorylation and Ubiquitylation Unit (MRC PPU) (School of Life Sciences, University of Dundee, Dundee, United Kingdom).

Analysis and identification of the matches were performed using a Basic Local Alignment Search Tool (BLAST) (https://blast.ncbi.nlm.nih.gov/Blast.cgi) (Altschul, Gish, Miller, Myers, & Lipman, 1990) in the National Center for Biotechnology Information nucleotide database (NCBI) (Coordinators, 2016)

2.8. Immunohistochemistry identification of FNDC5/irisin

The tissue sections around rats' upper molars, hPDL cells spheroids, hDPCs spheroids, hOBs spheroids, 2D cultured hPDL cells, hDPCs and hOBs were permeabilized with 0.1 % Triton X-100 (Sigma-Aldrich, Saint-Louis, Missouri, USA) in PBS for 5 min at room temperature. The samples were washed in PBS, blocked with 10 % normal goat serum (Abcam, Cambridge, United Kingdom) for 1 h prior to incubation with 1:200 diluted rabbit polyclonal anti-FNDC5 C-terminal antibody (ab181884; Abcam, Cambridge, United Kingdom) in 2 % normal goat serum overnight at 4 °C. For exclusion of the non-specific staining signals, negative control groups were incubated in 2 % normal goat serum without anti-FNDC5 antibody. On the following day, samples were washed 3 times in PBS and incubated with 1:500 diluted Alexa 488-conjugated goat anti-rabbit antibody (Invitrogen, Thermo Fisher Scientific, Carlsbad, CA, USA) in 4 % normal goat serum for 1 h in a humidified dark chamber at room temperature. The samples were washed 3 times in PBS, incubated with 300 nM 4′,6-diamidino-2-phenylindole (DAPI) (Sigma-Aldrich, Saint-Louis, Missouri, USA) for 20 min at room temperature, and covered by glass slips with Mowiol mounting medium made from Mowiol 4–88 (Sigma-Aldrich, Saint-Louis, Missouri, USA). Samples on the glass slides were kept in a dark chamber at room temperature until microscopic analysis.

FNDC5-expressing cells were imaged with Leica SP8 confocal microscope (Leica Microsystems CMS GmbH, Mannheim, Germany) using 405 nm and 488 nm excitation, and 420−480 nm and 500−550 nm emission filters for DAPI and Alexa Fluor 488, respectively. 3 images were captured for each group, the imaging settings were kept constant during individual assays.

2.9. ELISA assay

FNDC5/irisin secretion in hDPCs was quantified in culture media obtained after 1, 3, 7 and 14 days of culture by an FNDC5 ELISA Kit (Human): 96 Wells (Aviva Systems Biology, San Diego, CA, USA) following manufacturer's instructions. The plates were read at the wavelength of 450 nm using a spectrophotometer (BioTek, Winooski, USA), and the concentrations of FNDC5/irisin were determined by comparing the optical density (OD) values of the tested samples to that of the standard curve.

2.10. Statistics

All data obtained from qPCR and ELISA are presented as the mean ± standard deviation (SD). Statistical comparison between groups (control groups and treatment groups) was performed using unpaired Student's *t* tests as both normality tests and equality tests passed (SigmaPlot 14.0; Systat Software, San Jose, CA, USA). A probability of ≤ 0.05 was considered statistically significant. All experiments were performed in triplicates.

3. Results

3.1. FNDC5/irisin is expressed in rats' periodontium and dental pulp tissues and in hPDL cells, hDPCs and hOBs

A strong FNDC5/irisin immunofluorescence signal was detected both in rats' PDL (Fig. 1B, E, C, F) and dental pulp (Fig. 1B, C). However, only weak immunofluorescent signal was observed in the alveolar bone (Fig. 1B, C). The FNDC5/irisin immunofluorescent signal was found to be specific, as there was virtually no signal detectable from the negative control sample which lacked the primary antibody (Fig. 1H, I, K, L).

The PCR product corresponding to FNDC5/irisin was confirmed to be present in all tested cell types by DNA electrophoresis (Fig. 2A). Sequencing of the PCR product from hPDL cells revealed that the deduced sequence was identical to Homo sapiens fibronectin type III domain containing 5 (FNDC5), transcript variant 3 in GenBank (Accession number NM_001171940.2) (Fig. 2B).

The FNDC5/irisin protein was correspondingly identified in spheroids of hPDL cells (Fig. 3B, C, E, F), spheroids of hDPCs (Fig. 4B, C, E, F), spheroids of hOBs (Fig. 5B, C, E, F), 2D cultured hPDL cells (Fig. 6B and C), 2 D cultured hDPCs (Fig. 6H and I) and 2D cultured hOBs (Fig. 6N and O). Moreover, the intensity of the immunostained protein appeared to be localized in the cytoplasm of hPDL cells (Fig. 6B and C), hDPCs (Fig. 6H and I) and hOBs (Fig. 6N and O).

3.2. FNDC5/irisin expression is regulated in hPDL cells, hDPCs and hOBs

The potential autoregulation of the FNDC5/irisin expression was investigated by administration of recombinant human irisin, while

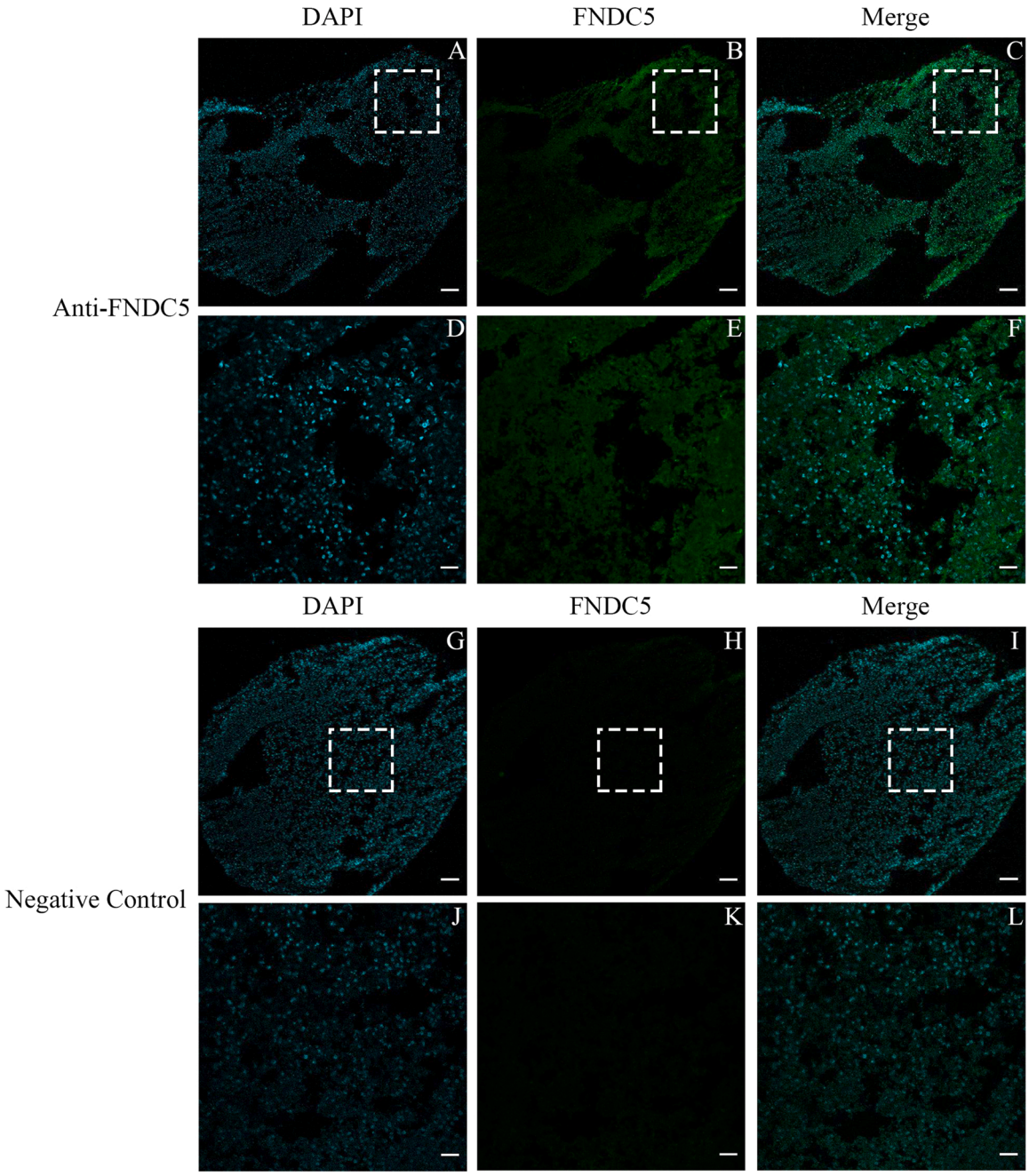


Fig. 3. Immunofluorescence detection of FNDC5/irisin in hPDL cell spheroids. Cryopreserved sections of spheroids were analyzed by immunofluorescence staining for FNDC5 (B, C, E and F), while negative control was not treated with anti-FNDC5 primary antibody (H, I, K and L). Nuclei were counterstained with DAPI (A, C, D, F, G, I, J and L). Merged images of DAPI and FNDC5 are shown in C, F, I and L. The white boxed areas are shown at a higher magnification (D, E, F, J, K and L). The images are representative of the respective groups. Scale bars in A, B, C, G, H and I represent 100 μm, scale bars in D, E, F, J, K and L represent 25 μm.

regulation was tested by administration of ATRA (Amengual et al., 2018) for 3 days. Both low and high concentrations of recombinant irisin significantly reduced FNDC5/irisin mRNA expression by 0.79 and 0.76 fold in hPDL cells compared to untreated control ($P = 0.008$ for 10 ng/mL, and $P = 0.014$ for 100 ng/mL) (Fig. 7A). Administration of ATRA significantly enhanced expression of FNDC5/irisin in hPDL cells by 2.8 ($P = 0.0003$ for 1 μM) and 1.7 fold ($P = 0.0002$ for 10 μM) compared to control (Fig. 7B).

Administration of the high dosage of recombinant irisin (100 ng/mL) significantly reduced expression of FNDC5/irisin ($P = 0.01$) by 0.5 fold in hDPCs compared to control, whereas the low dosage (10 ng/mL) had no effect ($P = 0.15$) (Fig. 7C). On the other hand, 1 μM ATRA enhanced FNDC5/irisin expression by approximately 3.1 fold ($P = 0.0004$) but the high dosage (10 μM) had no significant effect compared with control ($P = 0.25$) (Fig. 7D).

An inverse dose-dependent relationship was also observed in hOBs, where administration of 10 ng/mL recombinant irisin significantly enhanced the expression of FNDC5/irisin by nearly 4 fold in comparison to untreated control cells ($P = 0.01$), but 100 ng/mL did not affect the FNDC5/irisin mRNA expression ($P = 0.15$) (Fig. 7E). Both low and high concentrations of ATRA significantly decreased the FNDC5/irisin expression by 0.6 and 0.5n fold in hOBs ($P = 0.0008$ for 1 μM, and $P = 0.017$ for 10 μM) compared to control (Fig. 7F).

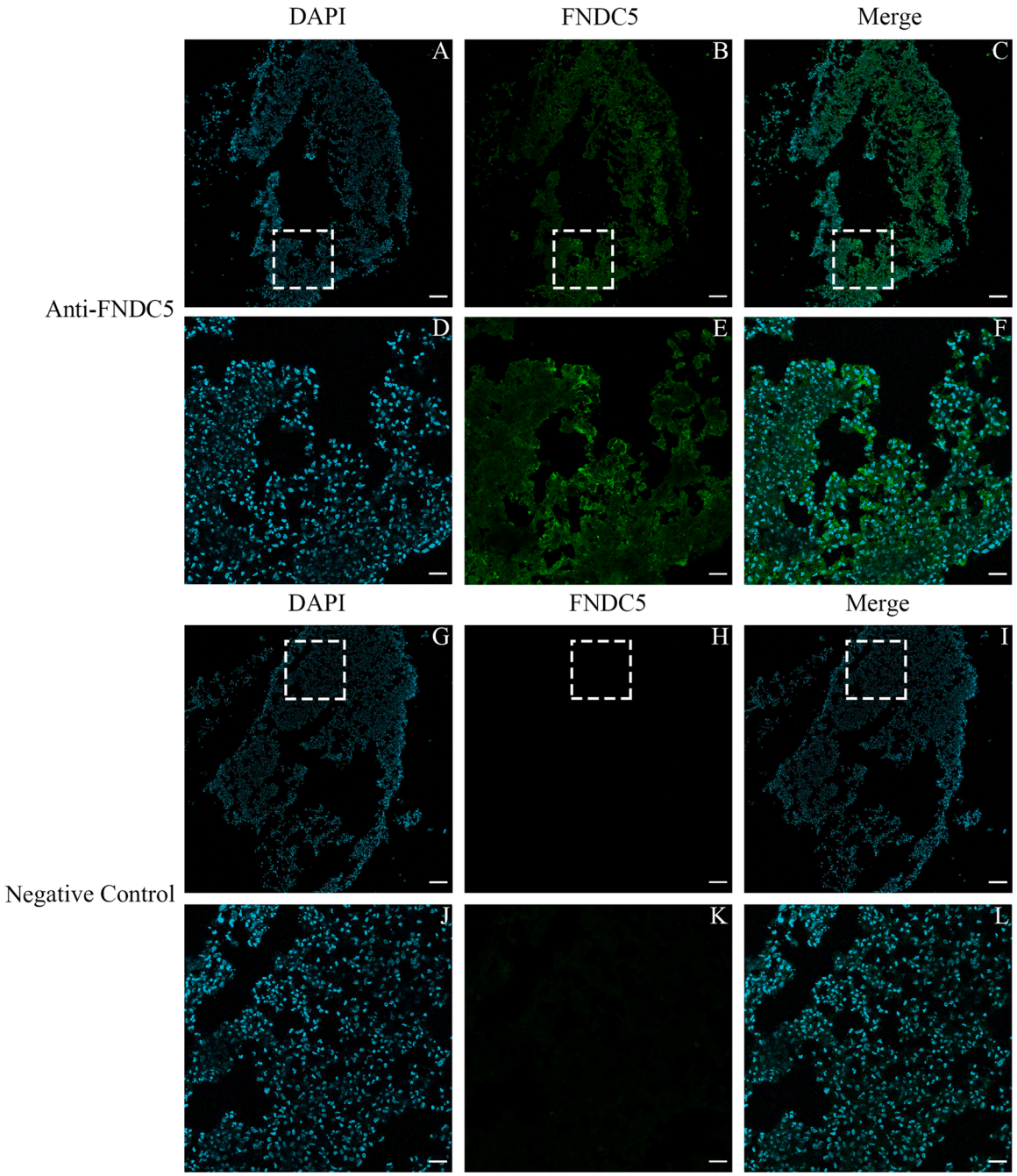


Fig. 4. Immunofluorescence detection of FNDC5/irisin in hDPCs spheroids. Cryopreserved sections of spheroids were analyzed by immunofluorescence staining for FNDC5 (B, E, C and F), while negative control was not treated with anti-FNDC5 primary antibody (H, I, K and L). Nuclei were counterstained with DAPI (A, C, D, F, G, I, J and L). Merged images of DAPI and FNDC5 are shown in C, F, I and L. The white boxed areas are shown at a higher magnification (D, E, F, J, K and L). The images are representative of the respective groups. Scale bars in A, B, C, G, H and I represent 100 μm, scale bars in D, E, F, J, K and L represent 25 μm.

3.3. The expression and secretion of FNDC5/irisin was affected by differentiation of hDPCs to odontoblast-like cells

The expression of FNDC5/irisin in hDPCs cultured with dexamethasone was significantly reduced by 0.22 fold at day 1 ($P = 0.007$) compared to control. At day 3, the expression of FNDC5/irisin was not different from control ($P = 0.17$), whereas the expression was significantly enhanced by 1.5 fold ($P = 0.0001$) at day 7 and 2.1 fold ($P = 0.0002$) at day14 compared to control (Fig. 8A). However, this enhancement of mRNA expression was not reflected in the levels of FNDC5/irisin secreted to cell culture medium over the same time period (Fig. 8B). No significant differences were observed at days 1, 3 and 7 ($P = 0.54$, $P = 0.15$, and $P = 0.69$, respectively), but at day 14 dexamethasone induced approximately 11 % decrease ($P = 0.017$) in the secretion of FNDC5/irisin compared to control (Fig. 8B).

4. Discussion

To the authors' best knowledge, the present research is the first to confirm that FNDC5/irisin is expressed in hPDL cells, hDPCs and hOBs. Moreover, a regulatory role of recombinant irisin and ATRA on FNDC5/irisin expression in hPDL cells and hDPCs was demonstrated. Finally, odontoblast-like differentiation of hDPCs might have an effect on the expression and secretion of FNDC5/irisin.

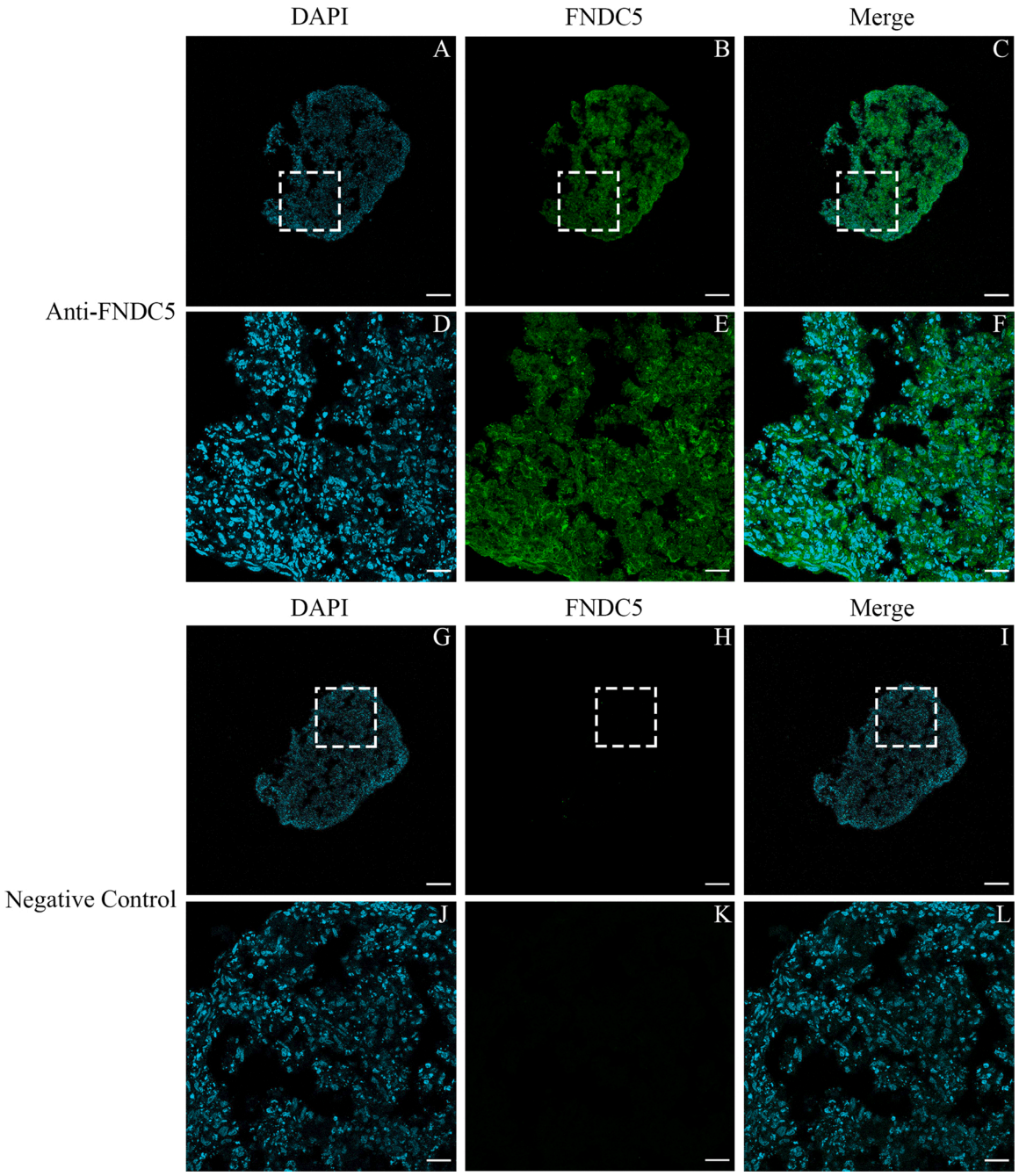


Fig. 5. Immunofluorescence detection of FNDC5/irisin in hOBs spheroids. Cryopreserved sections of spheroids were analyzed by immunofluorescence staining for FNDC5 (B, C, E and F), while negative control was not treated with anti-FNDC5 primary antibody (H, I, K and L). Nuclei were counterstained with DAPI (A, C, D, F, G, I, J and L). Merged images of DAPI and FNDC5 are shown in C, F, I and L. The white boxed areas are shown at a higher magnification (D, E, F, J, K and L). The images are representative of the respective groups. Scale bars in A, B, C, G, H and I represent 100 μm, scale bars in D, E, F, J, K and L represent 25 μm.

A FNDC5/irisin immunofluorescent signal was found in PDL tissues of rats. The sequence alignment of the amplified irisin product from hPDL cells matched with the human FNDC5 gene, which serves as evidence to confirm the expression of FNDC5/irisin in hPDL cells. According to Böstrom's study, FNDC5 comprises of a signal peptide, two fibronectin domains and one hydrophobic domain in structure (Boström et al., 2012). They found that the C-terminal region FNDC5 accumulated in cytoplasm, while the N-terminal region of FNDC5, which is termed as irisin, was proteolytically cleaved and released into circulation (Boström et al., 2012). Anti-FNDC5-C-terminal antibodies stained mainly the cytoplasm of 2D cultured hPDL cells, hDPCs and hOBs, which is in accordance with Boström et al.'s observations. Together with our previous findings suggesting that treatment with recombinant irisin enhanced both hPDL cells' and hOBs' growth, migration and osteogenic behavior (Pullisaar et al., 2019), the present findings could indicate that the FNDC5/irisin may play a role in periodontal regeneration.

Irisin is the first myokine that has been reported to be involved in mechano-transduction and could be regulated by mechanical stress (Boström et al., 2012; Kawao, Moritake, Tatsumi, & Kaji, 2018). In addition, irisin is released into blood in response to physical exercise and may have peripheral effects on various tissues (Varela-Rodríguez et al., 2016) as well as autocrine effect on skeletal muscles (Colaianni, Brunetti, Colucci, & Grano, 2018). It is widely accepted that high bone mass and strengthened bones can be achieved by physical activities, on the

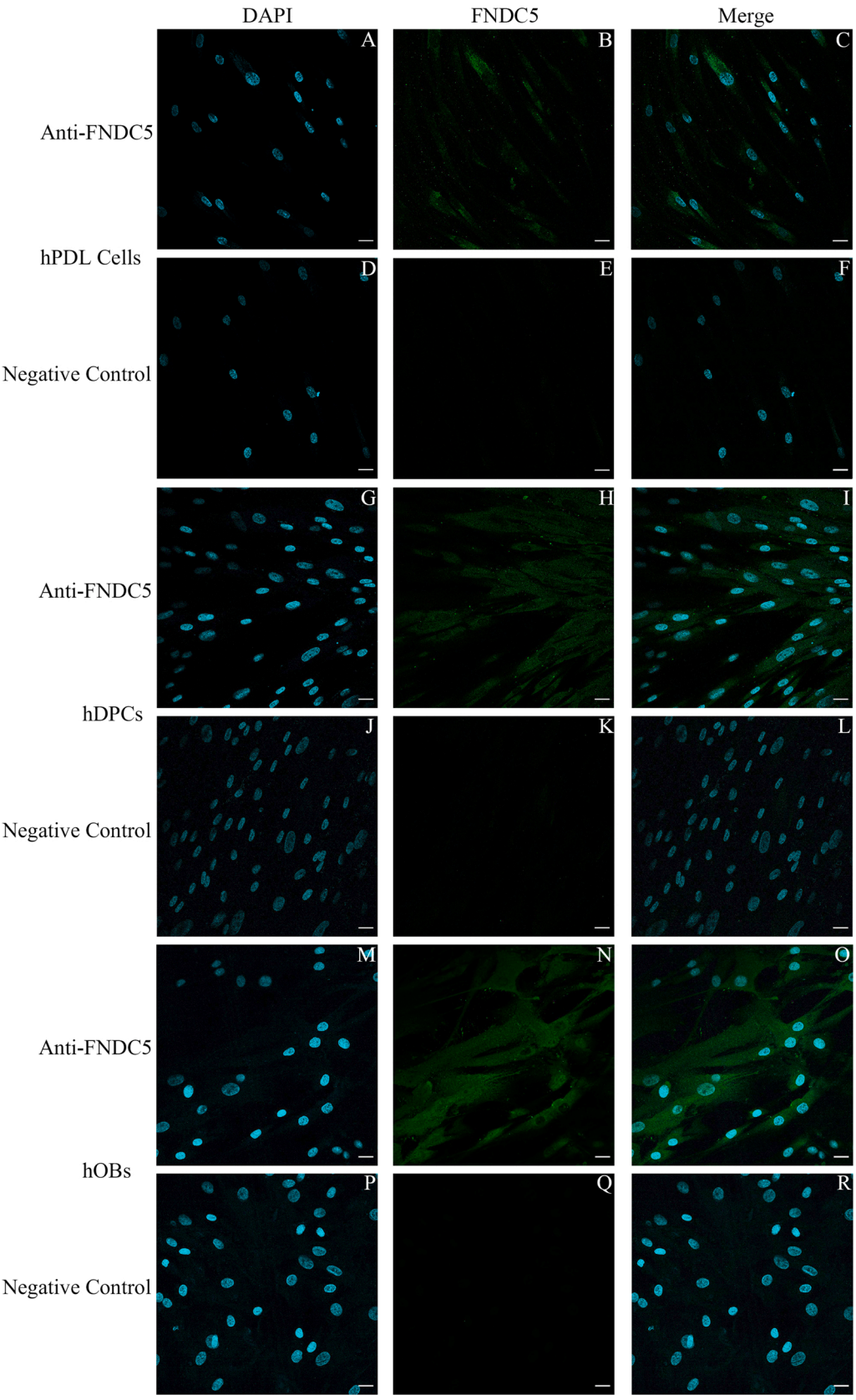


Fig. 6. Immunofluorescence detection of FNDC5/irisin in 2D cultured hPDL cells, hDPCs and hOBs. Cells were immunolabeled with anti-FNDC5 primary antibody (B, C, H, I, N and O), while negative control was not treated with primary anti-FNDC5 antibody (E, F, K, L, Q and R). Nuclei were counterstained with DAPI (A, C, D, F, G, I, J, L, M, O, P and R). Merged images of DAPI and FNDC5 are shown in C, F, I, L, O and R. The images are representative of the respective groups. Scale bar represents 25 μm.

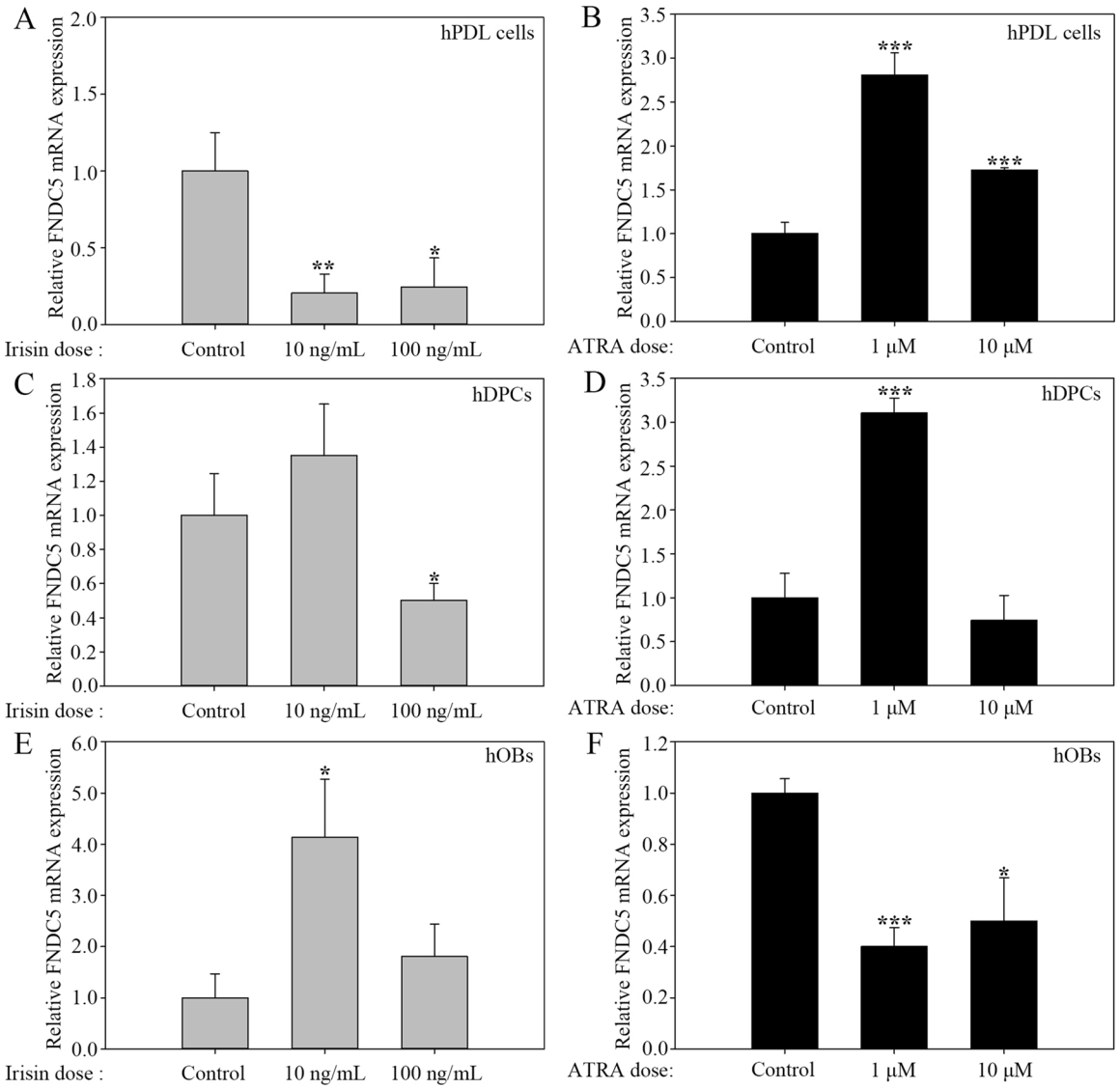


Fig. 7. mRNA expression levels of FNDC5/irisin in hPDL cells, hDPCs and hOBs treated with or without recombinant irisin (10 ng/mL, 100 ng/mL) and ATRA (1 μM, 10 μM). The relative mRNA expression levels of irisin were normalized to GAPDH. (*) $P < 0.05$; (**) $P < 0.01$; (***) $P < 0.001$ *vs* control group. All data present mean ± SD of 3 independent experiments.

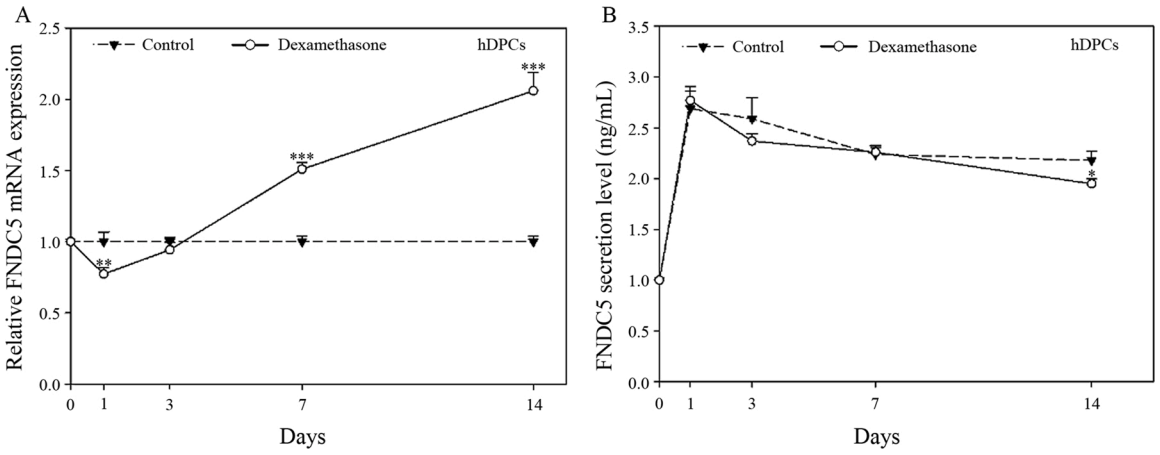


Fig. 8. Expression and secretion of FNDC5/irisin during odontoblast-like differentiation of hDPCs. (A) The mRNA expression levels of FNDC5/irisin from hDPCs over a 14-day odontoblast-like differentiation period. The expression was normalized to GAPDH, (**) $P < 0.01$; (***) $P < 0.001$ *vs* control group. (B) The secretion levels of FNDC5/irisin from hDPCs over a 14-day odontoblast-like differentiation period. (*) $P < 0.05$ *vs* control group. All data present mean ± SD of 3 independent experiments.

other hand, lack of physical activities or disuse of muscles result in severe bone loss (Chestnut, 1993; Colaianni et al., 2014). Likewise, healthy PDL helps to maintain bone mass of the tooth-supporting alveolar bone, whereas diseased periodontal tissues or loss of teeth will cause loss of load, thus resulting in irreversible bone resorption (Berkovitz, 2004; Bodic, Hamel, Lerouxel, Basle, & Chappard, 2005; Di Benedetto, Gigante, Colucci, & Grano, 2013). Therefore, PDL is situated in an environment that resembles that of skeletal muscles. Based on our results that both hPDL cells and rats' PDL sections expressed FNDC5/irisin, we can speculate that FNDC5/irisin expression may be regulated in response to mechanical stimuli of PDL.

In addition to a strong immunofluorescent signal from PDL, FNDC5/irisin was identified to be present in the rat pulp region and to lesser degree in the alveolar bone. We verified these findings by demonstrating that FNDC5/irisin was expressed in 3D spheroids generated from primary hPDL cells, hDPCs and hOBs, mimicking *in vivo* microenvironments (Fontoura et al., 2020; Schröder et al., 2020) as well as in 2D cultured cells. To the authors' knowledge, this is the first demonstration of FNDC5/irisin expression in 3D cultured cells *in vitro*. 2D monolayer cell culturing is the most common culture method, resulting in a homogeneous cell environment that is easy to control, analyze and sustain the ability to proliferate for most types of cells. However, cells are not generally considered to be kept in the natural microenvironment under such circumstances (Fennema, Rivron, Rouwkema, van Blitterswijk, & de Boer, 2013). 3D cultures provide cellular heterogeneity, nutrient and oxygen gradients, cell to cell interactions and matrix deposition so that the *in vivo* environment can be simulated *in vitro* and cells can be induced to behave in a natural environment (Ravi, Paramesh, Kaviya, Anuradha, & Solomon, 2015).

The FNDC5/irisin immunofluorescent signal was barely detected in rat alveolar bone. Preceding research has reported that irisin levels are positively correlated with bone mineral density (BMD) (Singhal et al., 2014; Wu et al., 2018). However, the rat samples in our study were obtained from the tissues around the molars located in the posterior maxilla, which contains lower BMD compared to anterior maxilla and mandible (Devlin, Horner, & Ledgerton, 1998). Moreover, positive correlations between irisin and BMD at different anatomical sites have also been reported (Colaianni et al., 2017), and can thus partly explain our observation. It has been demonstrated previously that murine bone tissues express FNDC5 (Zhang et al., 2017) and that recombinant irisin has a positive effect on proliferation and differentiation of osteoblasts *in vitro* (Pullisaar et al., 2019). However, our study is the first to confirm the expression of FNDC5/irisin in primary human osteoblasts.

To date, the molecular regulation of FNDC5/irisin expression remains largely unknown. FNDC5 is one of the target proteins for peroxisome proliferator-activated receptor-gamma coactivator 1 alpha (PGC-1α), and Boström et al. reported that the expression of PGC-1α stimulated the FNDC5 expression and the secretion of irisin (Boström et al., 2012). Administration of ATRA has been found to induce PGC-1α expression in differentiated 3T3-L1 adipocytes (Mercader et al., 2007) and enhance the gene expression of FNDC5 in C2C12 mouse myoblasts (Abedi-Taleb et al., 2019). We found that ATRA enhanced the expression of FNDC5/irisin in both hPDL cells and hDPCs. However, it attenuated the FNDC5/irisin expression in hOBs. Treatment with recombinant irisin reduced the FNDC5/irisin expression in hPDL cells and hDPCs, while it enhanced the FNDC5/irisin expression in hOBs. The converse effects of recombinant irisin and ATRA on hPDL cells and hDPCs *versus* hOBs in our study may be due to a cell type-specific effect of recombinant irisin and ATRA on the regulation of FNDC5/irisin expression.

Over the past years hDPCs have received broad attention in oral tissue engineering and regeneration owing to their ability to differentiate towards several cell types (Nuti et al., 2016). Dexamethasone treatment has been found to induce odontoblast-like differentiation of hDPCs as evidenced by enhanced expression of alkaline phosphatase (ALP), the major odontoblastic maker dentin sialophosphoprotein, reduced proliferation and enhanced mineralization (Alliot-Licht et al., 2005; Lim et al., 2016; Moretti, Duailibi, Martins, Santos, & Duailibi, 2017). In our study, we found the mRNA expression of FNDC5/irisin to be gradually enhanced in a time-dependent manner over a 14-day period of dexamethasone-induced odontoblast-like differentiation. Conversely, the secretion of FNDC5/irisin was found to be slightly reduced at day 14. Such lack of correlation between the change in FNDC5/irisin mRNA expression and protein secretion has previously been reported. (Roca-Rivada et al., 2013; Tian et al., 2004). Irisin, the secreted form of FNDC5, is proteolytically cleaved and released in response to physical stimulation. It is likely that while treatment with dexamethasone induced an enhanced mRNA expression of FNDC5/irisin in hDPCs, the translation and cleavage of irisin from FNDC5 and thus secretion from hDPCs was not affected.

In conclusion, FNDC5/irisin is expressed in hPDL cells, hDPCs, hOBs, rat PDL and rat dental pulp tissues. Further, FNDC5/irisin production and/or secretion from hPDL cells, hDPCs and hOBs is regulated, indicating that FNDC5/irisin may have autocrine, paracrine and endocrine effects in oral and bone tissues. Finally, the induced odontoblast-like differentiation of hDPCs appeared to affect both expression and secretion of FNDC5/irisin.

Authors' contributions

The conception and experimental design: YY, HP, MG, JER
Supervision: HP, JER
Performance of experiments: YY, MAL, CAH, MS, TXG
Analysis and interpretation of data: YY, HP, MAL, CAH, JER
Manuscript drafting and revision: YY, HP, MAL, CAH, MS, TXG, MG, JER
Final approval of the submitted version: YY, HP, MAL, CAH, MS, TXG, MG, JER

Declaration of Competing Interest

The authors declare that they have no known competing financial interests or personal relationships that could have appeared to influence the work reported in this paper.

Acknowledgments

This work was supported by the Research Council of Norway (project 287953) and Yang Yang (CSC number 201908420242) would like to thank China Scholarship Council (CSC) for personal grant.

References

Abedi-Taleb, E., Vahabi, Z., Sekhavati-Moghadam, E., Khedmat, L., Jazayeri, S., & Saboor-Yaraghi, A. A. (2019). Upregulation of FNDC5 gene expression in C2C12 cells after single and combined treatments of resveratrol and ATRA. *Lipids in Health and Disease, 18*(1), 181. https://doi.org/10.1186/s12944-019-1128-y

Alliot-Licht, B., Bluteau, G., Magne, D., Lopez-Cazaux, S., Lieubeau, B., Daculsi, G., … Guicheux, J. (2005). Dexamethasone stimulates differentiation of odontoblast-like cells in human dental pulp cultures. *Cell and Tissue Research, 321*(3), 391–400. https://doi.org/10.1007/s00441-005-1115-7

Altschul, S. F., Gish, W., Miller, W., Myers, E. W., & Lipman, D. J. (1990). Basic local alignment search tool. *Journal of Molecular Biology, 215*(3), 403–410. https://doi.org/10.1016/s0022-2836(05)80360-2

Amengual, J., Garcia-Carrizo, F. J., Arreguin, A., Musinovic, H., Granados, N., Palou, A., … Ribot, J. (2018). Retinoic acid increases fatty acid oxidation and irisin expression in skeletal muscle cells and impacts Irisin in vivo. *Cellular Physiology and Biochemistry, 46*(1), 187–202. https://doi.org/10.1159/000488422

Aydin, S., Aydin, S., Kuloglu, T., Yilmaz, M., Kalayci, M., Sahin, I., … Cicek, D. (2013). Alterations of irisin concentrations in saliva and serum of obese and normal-weight subjects, before and after 45 min of a Turkish bath or running. *Peptides, 50*, 13–18. https://doi.org/10.1016/j.peptides.2013.09.011

Aydin, S., Aydin, S., Kobat, M. A., Kalayci, M., Eren, M. N., Yilmaz, M., … Baydas, A. (2014). Decreased saliva/serum irisin concentrations in the acute myocardial infarction promising for being a new candidate biomarker for diagnosis of this pathology. *Peptides, 56*, 141–145. https://doi.org/10.1016/j.peptides.2014.04.002

Aydin, S., Kuloglu, T., Aydin, S., Kalayci, M., Yilmaz, M., Cakmak, T., … Ozercan, I. H. (2014). A comprehensive immunohistochemical examination of the distribution of

the fat-burning protein irisin in biological tissues. *Peptides, 61*, 130–136. https://doi.org/10.1016/j.peptides.2014.09.014

Bartold, P. M. (1991). Connective tissues of the periodontium. Research and clinical implications. *Australian Dental Journal, 36*(4), 255–268. https://doi.org/10.1111/j.1834-7819.1991.tb00720.x

Berkovitz, B. K. B. (2004). Periodontal ligament: Structural and clinical correlates. *Dental Update, 31*(1), 46–54. https://doi.org/10.12968/denu.2004.31.1.46

Bodic, F., Hamel, L., Lerouxel, E., Basle, M. F., & Chappard, D. (2005). Bone loss and teeth. *Joint, Bone, Spine, 72*(3), 215–221. https://doi.org/10.1016/j.jbspin.2004.03.007

Boström, P., Wu, J., Jedrychowski, M. P., Korde, A., Ye, L., Lo, J. C., … Spiegelman, B. M. (2012). A PGC1-alpha-dependent myokine that drives brown-fat-like development of white fat and thermogenesis. *Nature, 481*(7382), 463–468. https://doi.org/10.1038/nature10777

Chalisserry, E. P., Nam, S. Y., Park, S. H., & Anil, S. (2017). Therapeutic potential of dental stem cells. *Journal of Tissue Engineering, 8*. https://doi.org/10.1177/2041731417702531, 2041731417702531.

Chestnut, C. H. (1993). Bone mass and exercise. *The American Journal of Medicine, 95*(5, Supplement 1), S34–S36. https://doi.org/10.1016/0002-9343(93)90379-4

Colaianni, G., Brunetti, G., Colucci, S. C., & Grano, M. (2018). Myokine—Irisin—And its effects linking bone and muscle function. *Clinical Reviews in Bone and Mineral Metabolism, 16*(1), 16–21. https://doi.org/10.1007/s12018-017-9240-x

Colaianni, G., Cuscito, C., Mongelli, T., Oranger, A., Mori, G., Brunetti, G., … Grano, M. (2014). Irisin enhances osteoblast differentiation in vitro. *International Journal of Endocrinology, 2014*, Article 902186. https://doi.org/10.1155/2014/902186

Colaianni, G., Notarnicola, A., Sanesi, L., Brunetti, G., Lippo, L., Celi, M., … Grano, M. (2017). Irisin levels correlate with bone mineral density in soccer players. *Journal of Biological Regulators and Homeostatic Agents, 31*(4 suppl 1), 21–28.

Coordinators, N. R. (2016). Database resources of the national center for biotechnology information. *Nucleic Acids Research, 44*(D1), D7–D19. https://doi.org/10.1093/nar/gkv1290

Devlin, H., Horner, K., & Ledgerton, D. (1998). A comparison of maxillary and mandibular bone mineral densities. *The Journal of Prosthetic Dentistry, 79*(3), 323–327. https://doi.org/10.1016/S0022-3913(98)70245-8

Di Benedetto, A., Gigante, I., Colucci, S., & Grano, M. (2013). Periodontal disease: Linking the primary inflammation to bone loss. *Clinical & Developmental Immunology, 2013*, Article 503754. https://doi.org/10.1155/2013/503754

Feller, L., Khammissa, R. A. G., Schechter, I., Thomadakis, G., Fourie, J., & Lemmer, J. (2015). Biological events in periodontal ligament and alveolar bone associated with application of orthodontic forces. *The Scientific World Journal, 2015*, Article 876509. https://doi.org/10.1155/2015/876509

Fennema, E., Rivron, N., Rouwkema, J., van Blitterswijk, C., & de Boer, J. (2013). Spheroid culture as a tool for creating 3D complex tissues. *Trends in Biotechnology, 31*(2), 108–115. https://doi.org/10.1016/j.tibtech.2012.12.003

Fontoura, J. C., Viezzer, C., dos Santos, F. G., Ligabue, R. A., Weinlich, R., Puga, R. D., … Bonorino, C. (2020). Comparison of 2D and 3D cell culture models for cell growth, gene expression and drug resistance. *Materials Science and Engineering C, 107*, Article 110264. https://doi.org/10.1016/j.msec.2019.110264

Forouzanfar, M., Rabiee, F., Ghaedi, K., Beheshti, S., Tanhaei, S., Shoaraye Nejati, A., … Nasr-Esfahani, M. H. (2015). Fndc5 overexpression facilitated neural differentiation of mouse embryonic stem cells. *Cell Biology International, 39*(5), 629–637. https://doi.org/10.1002/cbin.10427

Kawao, N., Moritake, A., Tatsumi, K., & Kaji, H. (2018). Roles of Irisin in the linkage from muscle to bone during mechanical unloading in mice. *Calcified Tissue International, 103*(1), 24–34. https://doi.org/10.1007/s00223-018-0387-3

Lim, H. C., Nam, O. H., Kim, M. J., El-Fiqi, A., Yun, H. M., Lee, Y. M., … Kim, E. C. (2016). Delivery of dexamethasone from bioactive nanofiber matrices stimulates odontogenesis of human dental pulp cells through integrin/BMP/mTOR signaling pathways. *International Journal of Nanomedicine, 11*, 2557–2567. https://doi.org/10.2147/IJN.S97846

Lin, J. D., Jang, A. T., Kurylo, M. P., Hurng, J., Yang, F., Yang, L., … Ho, S. P. (2017). Periodontal ligament entheses and their adaptive role in the context of dentoalveolar joint function. *Dental Materials, 33*(6), 650–666. https://doi.org/10.1016/j.dental.2017.03.007

Livak, K. J., & Schmittgen, T. D. (2001). Analysis of relative gene expression data using real-time quantitative PCR and the 2(-Delta Delta C(T)) Method. *Methods, 25*(4), 402–408. https://doi.org/10.1006/meth.2001.1262

Mercader, J., Madsen, L., Felipe, F., Palou, A., Kristiansen, K., & Bonet, L. (2007). All-trans retinoic acid increases oxidative metabolism in mature adipocytes. *Cellular Physiology and Biochemistry, 20*(6), 1061–1072. https://doi.org/10.1159/000110717

Moretti, R.d. C., Duailibi, M. T., Martins, P. O., Santos, J. A.d., & Duailibi, S. E. (2017). Osteoinductive effects of preoperative dexamethasone in human dental pulp stem cells primary culture. *Future Science OA, 3*(3), FSO184. https://doi.org/10.4155/fsoa-2016-0083

Nuti, N., Corallo, C., Chan, B. M., Ferrari, M., & Gerami-Naini, B. (2016). Multipotent differentiation of human dental pulp stem cells: A literature review. *Stem Cell Reviews and Reports, 12*(5), 511–523. https://doi.org/10.1007/s12015-016-9661-9

Ozaki, S., Kaneko, S., Podyma-Inoue, K. A., Yanagishita, M., & Soma, K. (2005). Modulation of extracellular matrix synthesis and alkaline phosphatase activity of periodontal ligament cells by mechanical stress. *Journal of Periodontal Research Supplement, 40*(2), 110–117. https://doi.org/10.1111/j.1600-0765.2004.00782.x

Pullisaar, H., Colaianni, G., Lian, A. M., Vandevska-Radunovic, V., Grano, M., & Reseland, J. E. (2019). Irisin promotes growth, migration and matrix formation in human periodontal ligament cells. *Archives of Oral Biology, 111*, Article 104635. https://doi.org/10.1016/j.archoralbio.2019.104635

Rabiee, F., Forouzanfar, M., Ghazvini Zadegan, F., Tanhaei, S., Ghaedi, K., Motovali Bashi, M., … Nasr-Esfahani, M. H. (2014). Induced expression of Fndc5 significantly increased cardiomyocyte differentiation rate of mouse embryonic stem cells. *Gene, 551*(2), 127–137. https://doi.org/10.1016/j.gene.2014.08.045

Ravi, M., Paramesh, V., Kaviya, S. R., Anuradha, E., & Solomon, F. D. (2015). 3D cell culture systems: Advantages and applications. *Journal of Cellular Physiology, 230*(1), 16–26. https://doi.org/10.1002/jcp.24683

Roca-Rivada, A., Castelao, C., Senin, L. L., Landrove, M. O., Baltar, J., Belen Crujeiras, A., … Pardo, M. (2013). FNDC5/irisin is not only a myokine but also an adipokine. *PloS One, 8*(4), e60563. https://doi.org/10.1371/journal.pone.0060563

Schröder, M., Riksen, E. A., He, J., Skallerud, B. H., Møller, M. E., Lian, A.-M., … Reseland, J. E. (2020). Vitamin K2 modulates vitamin D-induced mechanical properties of human 3D bone spheroids in vitro. *JBMR Plus, 4*(9), e10394. https://doi.org/10.1002/jbm4.10394

Singhal, V., Lawson, E., Ackerman, K., Fazeli, P., Clarke, H., Lee, H., … Misra, M. (2014). Irisin levels are lower in young amenorrheic athletes compared with eumenorrheic athletes and non-athletes and are associated with bone density and strength estimates. *PloS One, 9*(6), Article e100218. https://doi.org/10.1371/journal.pone.0100218

Tian, Q., Stepaniants, S. B., Mao, M., Weng, L., Feetham, M. C., Doyle, M. J., … Hood, L. E. (2004). Integrated genomic and proteomic analyses of gene expression in mammalian cells. *Molecular & Cellular Proteomics, 3*(10), 960. https://doi.org/10.1074/mcp.M400055-MCP200

Varela-Rodríguez, B. M., Pena-Bello, L., Juiz-Valiña, P., Vidal-Bretal, B., Cordido, F., & Sangiao-Alvarellos, S. (2016). FNDC5 expression and circulating irisin levels are modified by diet and hormonal conditions in hypothalamus, adipose tissue and muscle. *Scientific Reports, 6*(1), 29898. https://doi.org/10.1038/srep29898

Villa, O., Wohlfahrt, J. C., Mdla, I., Petzold, C., Reseland, J. E., Snead, M. L., … Lyngstadaas, S. P. (2015). Proline-rich peptide mimics effects of enamel matrix derivative on rat oral mucosa incisional wound healing. *The Journal of Periodontology, 86*(12), 1386–1395. https://doi.org/10.1902/jop.2015.150207

Wu, L. F., Zhu, D. C., Tang, C. H., Ge, B., Shi, J., Wang, B. H., … Lei, S. F. (2018). Association of plasma Irisin with bone mineral density in a large Chinese population using an extreme sampling design. *Calcified Tissue International, 103*(3), 246–251. https://doi.org/10.1007/s00223-018-0415-3

Zhang, J., Valverde, P., Zhu, X., Murray, D., Wu, Y., Yu, L., … Chen, J. (2017). Exercise-induced irisin in bone and systemic irisin administration reveal new regulatory mechanisms of bone metabolism. *Bone Research, 5*, 16056. https://doi.org/10.1038/boneres.2016.56

Zhu, J., Wang, Y., Cao, Z., Du, M., Hao, Y., Pan, J., … He, H. (2020). Irisin promotes cementoblast differentiation via p38 MAPK pathway. *Oral Diseases, 26*(5), 974–982. https://doi.org/10.1111/odi.13307